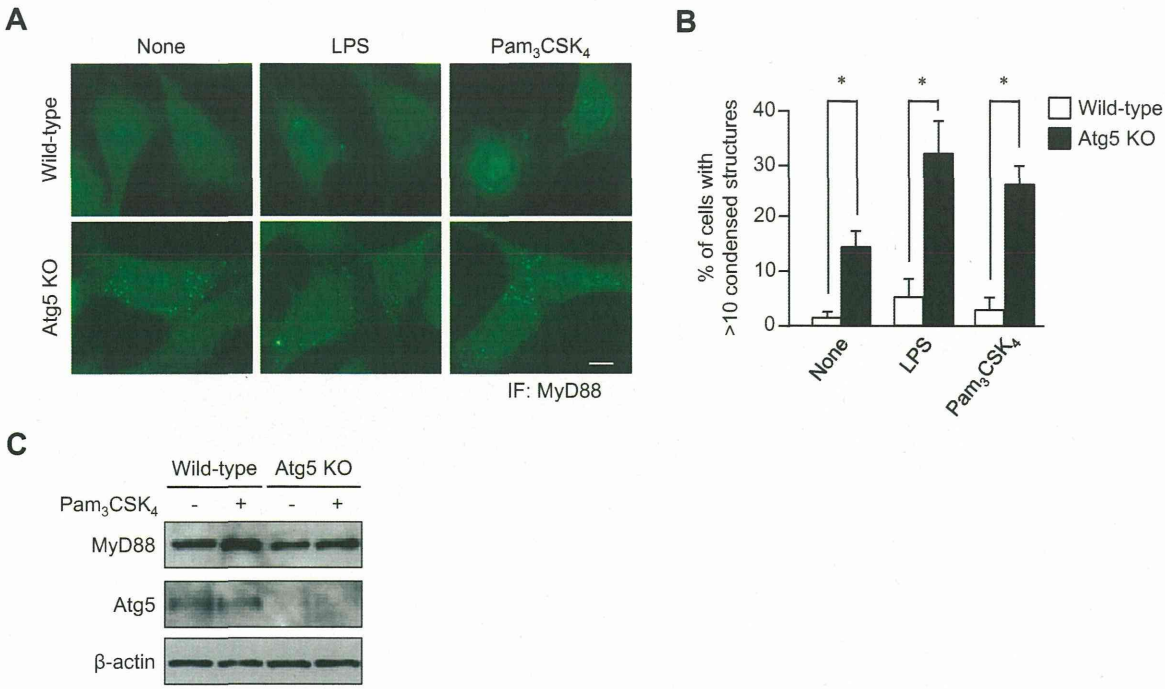

Fig. 1. Loss of Atg5 increases MyD88 condensed structures. (A) Wild-type and Atg5 KO MEFs were stimulated with LPS (1 μg/ml) or Pam_3CSK_4 (1 μg/ml) for 60 min. The cells were fixed and immunostained with anti-MyD88. Scale bar, 10 μm. (B) The percentage of cells with more than 10 microscopy-visible condensed structures of MyD88 was quantified by counting cells in 10 different images of microscopic fields that included at least 15 cells. Results, shown as means ± SD ($n = 3$), are representative of three independent experiments. (*$P < 0.01$). (C) Wild-type and Atg5 KO MEFs were stimulated with Pam_3CSK_4 (1 μg/ml) for 60 min and then subjected to immunoblot analysis using the indicated antibodies.

To determine whether Atg5 deficiency-induced MyD88 condensed structure formation is due to impairment of Atg5-mediated degradation of MyD88, we examined MyD88 protein expression in Atg5 KO MEFs. The level of MyD88 in Atg5 KO MEFs was the same as that in wild-type MEFs (Fig. 1C). Pam_3CSK_4 stimulation for 60 min slightly induced expression of MyD88 protein in wild-type and Atg5 KO MEFs (Fig. 1C). These results suggest that Atg5 suppresses the formation of MyD88 condensed structures, but it does not lead to degradation of MyD88.

3.2. MyD88-dependent signaling is not associated with LC3-dependent autophagic processes

Since the formation of MyD88 condensed structures is induced by LPS and Pam_3CSK_4, we investigated whether MyD88-dependent signaling is associated with autophagic processes. Generally, induction of LC3 puncta formation and conversion of LC3-I to LC3-II are known as a hallmark feature of autophagic flux [15]. We observed LC3 puncta structures and conversion of LC3-I to LC3-II induced by nutrient deprivation in wild-type MEFs but not in Atg5 KO MEFs (Fig. 2A and B). However, LPS stimulation did not induce LC3 puncta formation and LC3 conversion in wild-type and Atg5 KO MEFs (Fig. 2A and B). These results indicate that MyD88-dependent signaling is not correlated with LC3-dependent autophagic processes.

3.3. Atg5 interacts with MyD88

To examine the association between MyD88 and Atg5, coimmunoprecipitation analysis was performed. We found that Atg5 could interact with MyD88 (Fig. 3). This observation suggests that Atg5 interacts with MyD88 and then mediates the suppressive effect on formation of MyD88 condensed structures.

3.4. Atg5 regulates MyD88-dependent signaling

We have shown that the loss of Atg5 increases the formation of MyD88 condensed structures (Fig. 1A). Since condensed structures of MyD88 have been regarded as signaling complexes [9,10], we speculated that Atg5 exerts some physiological effects on formation of MyD88–TRAF6 signaling complex induced by TLR stimulation. To examine the effect of Atg5 on formation of MyD88–TRAF6 complex, we applied a biochemical approach utilizing MyD88 *C*-terminally fused to GyrB, which is known to dimerize upon binding with the *Streptomyces* product coumermycin [24]. In cells stably expressing MyD88–GyrB, coumermycin can activate signaling pathways similar to TLR signaling pathways through recruitment of TRAF6 to MyD88–GyrB [25]. Consistent with the results of a previous study [25], TRAF6 was co-immunoprecipitated with MyD88–GyrB after coumermycin treatment in wild-type and Atg5 KO MEFs (Fig. 4A). Interestingly, compared with wild-type MEFs, co-immunoprecipitated TRAF6 upon coumermycin treatment was obviously increased in Atg5 KO MEFs (Fig. 4A). These results indicate that Atg5 suppresses the formation of MyD88–TRAF6 signaling complex induced by TLR stimulation.

We next investigated whether Atg5 exerts downregulatory effects on the MyD88-mediated signaling pathway, since Atg5 inhibits its formation of the MyD88–TRAF6 signaling complex. Unexpectedly, Pam_3CSK_4-induced activation of p38, JNK, ERK and Akt was decreased in Atg5 KO MEFs compared with that in wild-type MEFs (Fig. 4B). On the other hand, Pam_3CSK_4-induced activation of NF-κB p65 and degradation of IκBα were enhanced in Atg5 KO MEFs compared with those in wild-type MEFs (Fig. 4B). The distinct regulatory effect of Atg5 on activation of MAPKs and NF-κB was also observed in wild-type and Atg5 KO MEFs after stimulation with LPS (Fig. S1). These results suggest that Atg5 has a downregulatory effect on activation of NF-κB signaling, whereas it has an upregulatory effect on MAPKs and Akt.

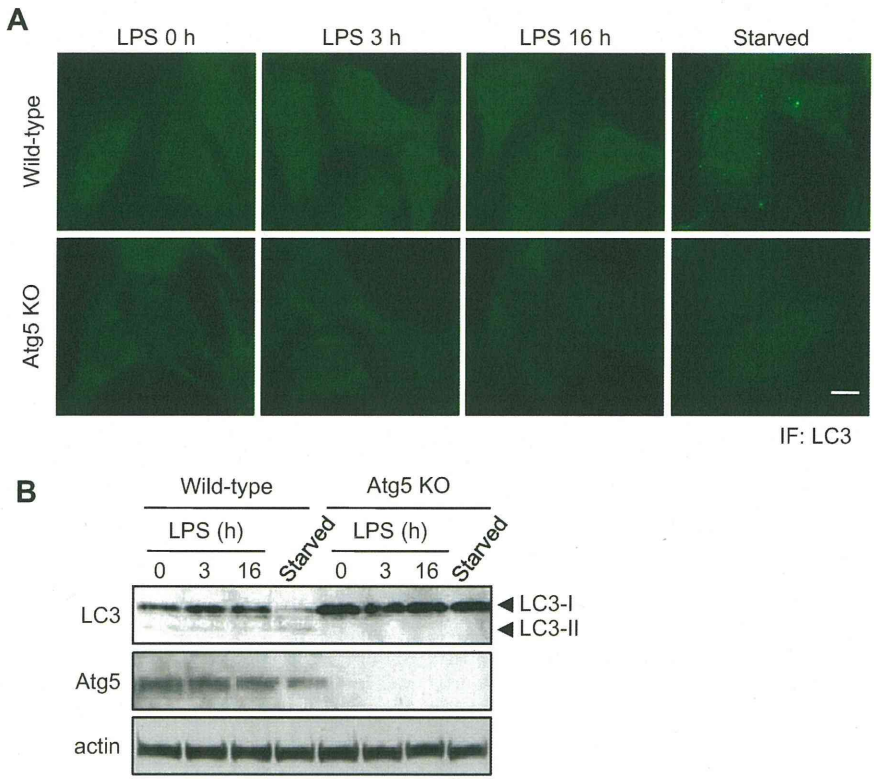

Fig. 2. TLR stimulation does not induce LC3-dependent autophagy. (A) Wild-type and Atg5 KO MEFs were stimulated with LPS (1 μg/ml) for the indicated periods. Alternatively, cells were cultured in DMEM without amino acids and serum for 16 h (starved). The cells were fixed and immunostained with anti-LC3. Scale bar, 10 μm. (B) Wild-type and Atg5 KO MEFs were stimulated with LPS (1 μg/ml) for the indicated periods. Alternatively, cells were cultured in DMEM without amino acids and serum for 3 h (starved). Cell lysates were analyzed by immunoblotting with indicated antibodies.

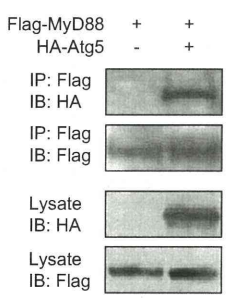

Fig. 3. Atg5 interacts with MyD88. HEK293T cells were transfected with Flag-MyD88 together with HA-Atg5. Cell lysates were immunoprecipitated with anti-Flag antibody and then subjected to immunoblotting analysis using anti-HA or anti-Flag antibodies.

4. Discussion

In the present study, we revealed that the autophagy-related protein Atg5 suppresses the formation of MyD88 condensed structures in the cytoplasm. We also obtained evidence that Atg5 inhibits formation of the MyD88–TRAF6 signaling complex induced by TLR stimulation, which ultimately limits the activation of NF-κB p65 and degradation of IκBα. Interestingly, Atg5 does not inhibit the activation of p38, JNK, ERK and Akt. These findings suggest that Atg5 may more preferentially inhibit activation of TAK1, which mediates the NF-κB signaling downstream of TRAF6. It is currently understood that TRAF6-generated unanchored polyubiquitin chains directly activate TAK1 but not MAPKs and Akt [6]. Therefore, Atg5 may suppress the formation of TRAF6-synthesized free polyubiquitin chains as well as the MyD88–TRAF6 signaling complex and exert a modulatory effect on MyD88-mediated signal transduction.

We found that endogenous MyD88 was already present as condensed structures in Atg5 KO MEFs. Although MyD88 condensed structures have been regarded as signaling complexes or myddosomes [9,10], activation of several signaling events, such as phosphorylation of NF-κB p65, was not observed. Therefore, it is possible that MyD88 is normally present as inactive condensed structures in the cytoplasm, but the formation of the structures is tightly regulated by Atg5.

Recent studies have indicated that each Atg controls certain types of cellular response through association with signaling molecules. Atg5 and the conjugate of Atg5–Atg12 associate with IFN-β promoter stimulator 1 (IPS-1) and retinoic acid-inducible gene I (RIG-I), essential molecules for immunostimulatory RNA (isRNA)-mediated signaling [26]. This association suppresses the interaction between IPS-1 and RIG-I, leading to inhibition of isRNA-mediated innate immune response [26]. In the case of Atg9a, it co-localizes with cytoplasmic punctate structures of stimulator of interferon genes (STING) and TANK-binding kinase 1 (TBK1), which are critical signaling molecules for double-stranded DNA (dsDNA)-induced signaling [27]. Subsequent characterization by electron microscopy revealed that punctate structures of STING induced by dsDNA do not have the morphological characteristics of autophagosomes, suggesting that Atg9a does not lead to autophagic degradation of STING [27]. However, interestingly, the loss of Atg9a greatly enhanced dsDNA-induced formation of punctate structures of STING and TBK1, resulting in activation of the innate immune response [27]. Therefore, it is possible that Atg9a regulates dsDNA-induced innate immune response independently of

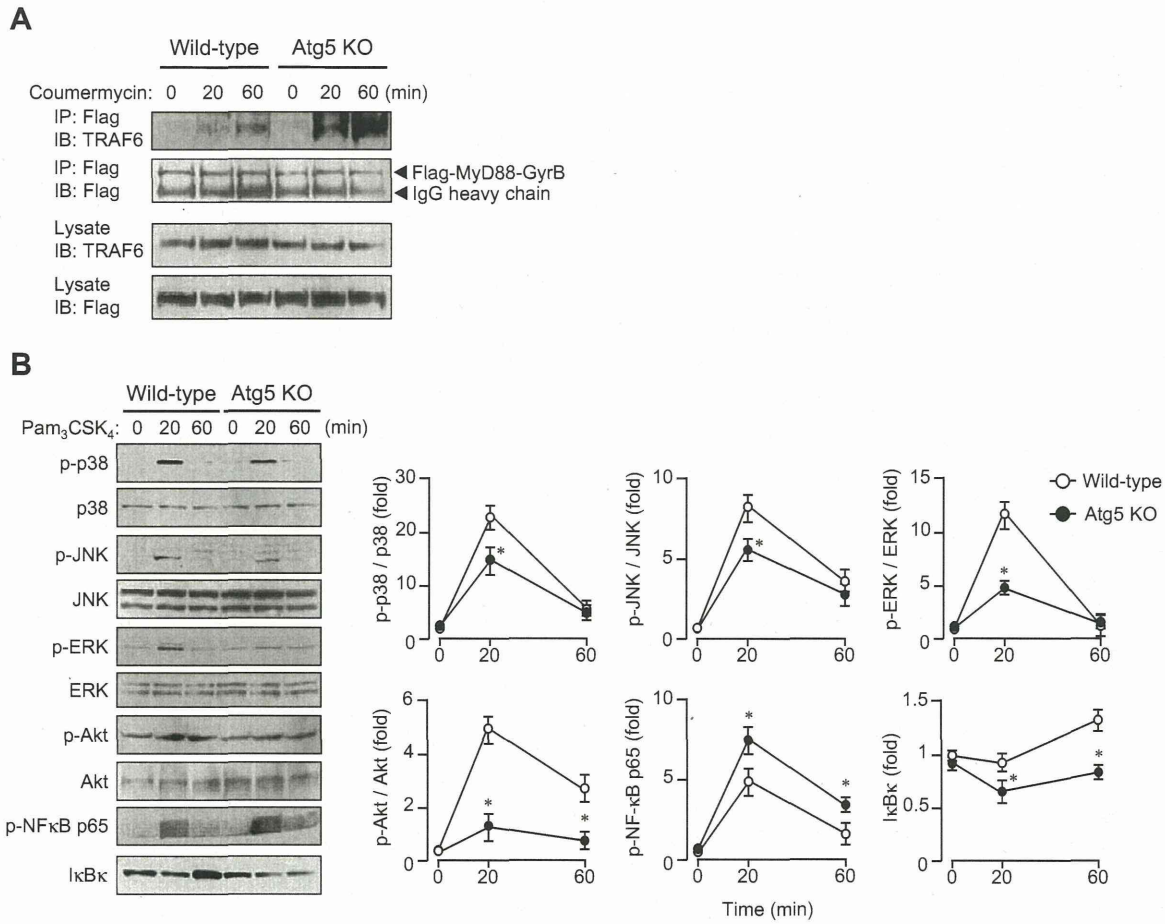

Fig. 4. Effect of Atg5 on signal transduction induced by TLR stimulation. (A) Wild-type and Atg5 KO MEFs stably expressing Flag-MyD88-GyrB were stimulated with coumermycin (1 μM) for the indicated periods. Cell lysates were immunoprecipitated with anti-Flag antibody and then subjected to immunoblotting analysis using anti-TRAF6 or anti-Flag antibodies. (B) Wild-type and Atg5 KO MEFs were stimulated with Pam_3CSK_4 (1 μg/ml) for the indicated periods. Cell lysates were subjected to immunoblotting analysis using the indicated antibodies. Densitometric quantification was performed on all of the immunoblot bands. Each value of p-p38, p-JNK, p-ERK and p-Akt was normalized to each level of total p38, total JNK, total ERK and total Akt, respectively. Results are expressed as means ± SD of three independent experiments and as fold increases by taking the control values (wild-type, 0 min) as 1. (*$P < 0.01$, for comparison with the wild-type group).

autophagic processes [27]. The present study demonstrated that the loss of Atg5 enhanced MyD88 condensed structure formation and several MyD88-mediated signaling events. Atg5 could interact with MyD88, but it did not induce MyD88 degradation. Moreover, activation of MyD88-dependent signaling by LPS stimulation did not induce LC3 punctate formation and LC3 conversion. These observations suggest that the regulatory effect of Atg5 on MyD88-dependent signaling may be exerted through association with MyD88, but not through autophagic processes.

The present study highlights a novel role of Atg5 in the regulation of formation of MyD88 condensed structures and MyD88-dependent signal transduction. Given that excess activation of MyD88-mediated responses induces inflammatory disorders [28], Atg5 may function as one of the essential fine-tuners of MyD88-dependent signaling.

Acknowledgments

We are grateful to Prof. N. Mizushima (Tokyo University, Tokyo, Japan) for providing cells and expression plasmids. This work was supported by a Grant-in-Aid for Young Scientists (B; 23792158 to M. Inomata) provided by the Ministry of Education, Culture, Sports, Science and Technology, Japan. This work was also supported by a Grant-in-Aid for Scientific Research (B; 23390431 to T. Into) from the Japan Society for the Promotion of Science (JSPS).

Appendix A. Supplementary data

Supplementary data associated with this article can be found, in the online version, at http://dx.doi.org/10.1016/j.bbrc.2013.06.094.

References

[1] H. Wesche, W.J. Henzel, W. Shillinglaw, S. Li, Z. Cao, MyD88: an adaptor that recruits IRAK to the IL-1 receptor complex, Immunity 7 (1997) 837–847.
[2] R. Medzhitov, P. Preston-Hurlburt, E. Kopp, A. Stadlen, C. Chen, S. Ghosh, C.A. Janeway Jr., MyD88 is an adaptor protein in the hToll/IL-1 receptor family signaling pathways, Mol. Cell 2 (1998) 253–258.
[3] M. Muzio, J. Ni, P. Feng, V.M. Dixit, IRAK (Pelle) family member IRAK-2 and MyD88 as proximal mediators of IL-1 signaling, Science 278 (1997) 1612–1615.
[4] S.C. Lin, Y.C. Lo, H. Wu, Helical assembly in the MyD88–IRAK4–IRAK2 complex in TLR/IL-1R signalling, Nature 465 (2010) 885–890.
[5] Z.J. Chen, Ubiquitin signalling in the NF-κB pathway, Nat. Cell Biol. 7 (2005) 758–765.
[6] Z.P. Xia, L. Sun, X. Chen, G. Pineda, X. Jiang, A. Adhikari, W. Zeng, Z.J. Chen, Direct activation of protein kinases by unanchored polyubiquitin chains, Nature 461 (2009) 114–119.
[7] S. Akira, S. Uematsu, O. Takeuchi, Pathogen recognition and innate immunity, Cell 124 (2006) 783–801.
[8] L.A. O'Neill, A.G. Bowie, The family of five: TIR-domain-containing adaptors in Toll-like receptor signalling, Nat. Rev. Immunol. 7 (2007) 353–364.
[9] T. Kawai, S. Sato, K.J. Ishii, C. Coban, H. Hemmi, M. Yamamoto, K. Terai, M. Matsuda, J. Inoue, S. Uematsu, O. Takeuchi, S. Akira, Interferon-α induction through Toll-like receptors involves a direct interaction of IRF7 with MyD88 and TRAF6, Nat. Immunol. 5 (2004) 1061–1068.

[10] J.C. Kagan, R. Medzhitov, Phosphoinositide-mediated adaptor recruitment controls Toll-like receptor signaling, Cell 125 (2006) 943–955.
[11] T. Nishiya, E. Kajita, T. Horinouchi, A. Nishimoto, S. Miwa, Distinct roles of TIR and non-TIR regions in the subcellular localization and signaling properties of MyD88, FEBS Lett. 581 (2007) 3223–3229.
[12] F. Jaunin, K. Burns, J. Tschopp, T.E. Martin, S. Fakan, Ultrastructural distribution of the death-domain-containing MyD88 protein in HeLa cells, Exp. Cell Res. 243 (1998) 67–75.
[13] T. Into, M. Inomata, S. Niida, Y. Murakami, K. Shibata, Regulation of MyD88 aggregation and the MyD88-dependent signaling pathway by sequestosome 1 and histone deacetylase 6, J. Biol. Chem. 285 (2010) 35759–35769.
[14] N. Mizushima, M. Komatsu, Autophagy: renovation of cells and tissues, Cell 147 (2011) 728–741.
[15] D.J. Klionsky, F.C. Abdalla, H. Abeliovich, et al., Guidelines for the use and interpretation of assays for monitoring autophagy, Autophagy 8 (2012) 445–544.
[16] M. Tsukada, Y. Ohsumi, Isolation and characterization of autophagy-defective mutants of *Saccharomyces cerevisiae*, FEBS Lett. 333 (1993) 169–174.
[17] D.J. Klionsky, J.M. Cregg, W.A. Dunn Jr., S.D. Emr, Y. Sakai, I.V. Sandoval, A. Sibirny, S. Subramani, M. Thumm, M. Veenhuis, Y. Ohsumi, A unified nomenclature for yeast autophagy-related genes, Dev. Cell 5 (2003) 539–545.
[18] N. Mizushima, Y. Ohsumi, T. Yoshimori, Autophagosome formation in mammalian cells, Cell Struct. Funct. 27 (2002) 421–429.
[19] Y. Ohsumi, Molecular dissection of autophagy: two ubiquitin-like systems, Nat. Rev. Mol. Cell Biol. 2 (2001) 211–216.
[20] T. Into, M. Inomata, M. Nakashima, K. Shibata, H. Häcker, K. Matsushita, Regulation of MyD88-dependent signaling events by S nitrosylation retards Toll-like receptor signal transduction and initiation of acute-phase immune responses, Mol. Cell. Biol. 28 (2008) 1338–1347.
[21] A. Kuma, M. Hatano, M. Matsui, A. Yamamoto, H. Nakaya, T. Yoshimori, Y. Ohsumi, T. Tokuhisa, N. Mizushima, The role of autophagy during the early neonatal starvation period, Nature 432 (2004) 1032–1036.
[22] M. Inomata, S. Niida, K. Shibata, T. Into, Regulation of Toll-like receptor signaling by NDP52-mediated selective autophagy is normally inactivated by A20, Cell. Mol. Life Sci. 69 (2012) 963–979.
[23] W.X. Ding, X.M. Yin, Sorting, recognition and activation of the misfolded protein degradation pathways through macroautophagy and the proteasome, Autophagy 4 (2008) 141–150.
[24] M.A. Farrar, J. Alberol-Ila, R.M. Perlmutter, Activation of the Raf-1 kinase cascade by coumermycin-induced dimerization, Nature 383 (1996) 178–181.
[25] H. Häcker, V. Redecke, B. Blagoev, I. Kratchmarova, L.C. Hsu, G.G. Wang, M.P. Kamps, E. Raz, H. Wagner, G. Häcker, M. Mann, M. Karin, Specificity in Toll-like receptor signalling through distinct effector functions of TRAF3 and TRAF6, Nature 439 (2006) 204–207.
[26] N. Jounai, F. Takeshita, K. Kobiyama, A. Sawano, A. Miyawaki, K.Q. Xin, K.J. Ishii, T. Kawai, S. Akira, K. Suzuki, K. Okuda, The Atg5–Atg12 conjugate associates with innate antiviral immune responses, Proc. Natl. Acad. Sci. USA 104 (2007) 14050–14055.
[27] T. Saitoh, N. Fujita, T. Hayashi, K. Takahara, T. Satoh, H. Lee, K. Matsunaga, S. Kageyama, H. Omori, T. Noda, N. Yamamoto, T. Kawai, K. Ishii, O. Takeuchi, T. Yoshimori, S. Akira, Atg9a controls dsDNA-driven dynamic translocation of STING and the innate immune response, Proc. Natl. Acad. Sci. USA 106 (2009) 20842–20846.
[28] F.Y. Liew, D. Xu, E.K. Brint, L.A. O'Neill, Negative regulation of Toll-like receptor-mediated immune responses, Nat. Rev. Immunol. 5 (2005) 446–458.

Reduced Surface Expression of TLR4 by a V254I Point Mutation Accounts for the Low Lipopolysaccharide Responder Phenotype of BALB/c B Cells

Hiroki Tsukamoto,*,† Kenji Fukudome,* Shoko Takao,* Naoko Tsuneyoshi,* Shoichiro Ohta,‡ Yoshinori Nagai,§ Hideyuki Ihara,† Kensuke Miyake,¶ Yoshitaka Ikeda,† and Masao Kimoto*

LPS is recognized by TLR4 and radioprotective 105 kDa in B cells. Susceptibility to LPS in murine B cells is most closely linked to the locus containing the *TLR4* gene. However, the molecular mechanism underlying genetic control of LPS sensitivity by this locus has not been fully elucidated. In this study, we revealed that C57BL/6 (B6) B cells respond to mAb-induced, TLR4-specific signals stronger than BALB/c (BALB) B cells, as assessed by proliferation and upregulation of CD69 and CD86. In contrast, BALB B cells were not hyporesponsive to agonistic anti–radioprotective 105 kDa mAb or the TLR9 agonist CpG. Although the level of *TLR4* mRNA in BALB B cells was comparable with that in B6 B cells, surface TLR4 expression in BALB B cells was lower than that in B6 B cells. This lower surface expression of BALB TLR4 was also observed when HEK293 and Ba/F3 cells were transfected with a BALB TLR4 expression construct. We identified a V254I mutation as the responsible single nucleotide polymorphism for lower surface expression of BALB TLR4. Furthermore, cotransfection of myeloid differentiation factor-2 increased BALB TLR4 expression, although it was still lower than B6 TLR4 expression. In concordance with reduced expression, Ba/F3 cells transfected with BALB TLR4 and myeloid differentiation factor-2 were hyporesponsive compared with those with B6 TLR4, as assessed by LPS-induced NF-κB activation. In conclusion, we revealed that LPS sensitivity is genetically controlled by the level of surface TLR4 expression on B cells. A V254I mutation accounts for the LPS hyporesponsive phenotype of BALB B cells. ***The Journal of Immunology*****, 2013, 190: 195–204.**

B cells are important immune cells as producers of Ab against pathogens and also play a role in inducing adaptive immunity as APCs (1). Various pathogen-associated molecules activate B cells via TLRs (2, 3). Among them, LPS, a major cell-wall component of Gram-negative bacteria, is a potent mitogen for B cells in mice (2, 3). B cells recognize LPS via the TLR4/myeloid differentiation factor-2 (MD-2) complex, resulting in cell activation, polyclonal proliferation, and Ab production (4). In addition, the TLR4 homologous receptor, radioprotective 105 kDa (RP105), has been reported to be involved in LPS recognition (5).

TLR4 is an indispensable innate immune receptor for recognition of LPS (4). With the help of its associate molecule MD-2 (6), TLR4 transmits activation signals caused by LPS via an MyD88-dependent and Toll/IL-1R domain–containing adapter-inducing IFN-β–dependent pathway (7). MD-2 directly binds to LPS via its hydrophobic binding pocket in concert with TLR4 (8). *TLR4*-deficient mice, as well as *MD-2*–deficient mice, are unresponsive to LPS and succumb to Gram-negative bacterial infection (4, 6). The surface localization of TLR4 is regulated by a complex mechanism, in which chaperone-like molecules are involved, that varies among TLR4-expressing cell types (6, 9, 10). MD-2 plays a role in transporting TLR4 to the cell surface (6, 11, 12), although it has been reported to be dispensable in dendritic cells and macrophages (11, 13). Coexpression of MD-2 enhances surface TLR4 levels in HEK293 cells (11, 12).

RP105 is homologous to TLR4 in that it is composed of leucine-rich repeat (LRR) motifs (14) and associates with MD-1, an MD-2 homolog (15). We previously demonstrated that *RP105*$^{-/-}$ (5) and *MD-1*$^{-/-}$ mice (15) are hyporesponsive to LPS challenge. Agonistic anti-RP105 mAbs induce robust activation of B cells (14, 16). These data suggest the involvement of RP105 in LPS-induced B cell activation. Recent crystallography experiments demonstrated that the MD-1 binding pocket does not accommodate LPS (17), although it was able to bind lipid IVa, a tetra-acylated LPS analog (18). The role of RP105 has been considered to extend beyond LPS recognition, because RP105 deficiency also limits the signaling events driven by TLR2 ligands that are structurally unrelated to LPS (19, 20).

*Department of Immunology, Saga Medical School, Saga 849-8501, Japan; †Division of Molecular Cell Biology, Department of Biomolecular Sciences, Saga University Faculty of Medicine, Saga 849-8501, Japan; ‡Department of Laboratory Medicine, Saga Medical School, Saga 849-8501, Japan; §Department of Immunobiology and Pharmacological Genetics, Graduate School of Medicine and Pharmaceutical Science for Research, University of Toyama, Toyama 930-0194, Japan; and ¶Division of Infectious Genetics, Department of Microbiology and Immunology, The Institute of Medical Science, University of Tokyo, Minato-ku, Tokyo 108-8639, Japan

Received for publication April 9, 2012. Accepted for publication November 1, 2012.

This work was supported by the Grants-in-Aid for Scientific Research from the Ministry of Education, Culture, Sports, Science and Technology of the Japanese Government (Grant 24790112 to H.T., Grant 22591064 to K.F., Grant 21590538 to M.K.).

Address correspondence to Dr. Hiroki Tsukamoto, Department of Immunology, Saga Medical School, 5-1-1 Nabeshima, Saga 849-8501, Japan. E-mail address: tsukamoh@cc.saga-u.ac.jp

The online version of this article contains supplemental material.

Abbreviations used in this article: B6, C57BL/6; BALB, BALB/c; Bio, biotinylated; BMDC, bone marrow–derived dendritic cell; BMM, bone marrow–derived macrophage; CM, conditioned medium; LRR, leucine-rich repeat; MD-2, myeloid differentiation factor-2; MFI, mean fluorescence intensity; PRAT4A, protein associated with TLR4; RP105, radioprotective 105 kDa; SNP, single nucleotide polymorphism; stv, streptavidin; TLR4C, C-terminal half of TLR4; TLR4N, N-terminal half of TLR4; wt, wild-type.

www.jimmunol.org/cgi/doi/10.4049/jimmunol.1201047

Susceptibility to LPS challenge is associated with genetic variations in mice (21–24) and humans (25). Allelic mutations of the *lps* locus in the C57BL/10ScCr and C3H/HeJ mutant strains of mice are known to completely abrogate the immune response to LPS (24). The *TLR4* gene was identified as the responsible *lps* gene by positional cloning experiments (24), which was confirmed by generation of *TLR4*$^{-/-}$ mice (4). In addition to these LPS unresponsive strains, C57BL/6 (B6) B cells have been known to be good responders to LPS, whereas BALB/c (BALB) B cells are known to be poor responders (21, 22). A genome-wide search implicated the locus containing the *TLR4* and *MHC class II* genes as major genetic factors controlling B cell responsiveness to LPS (22). Genetic studies using congenic strains of mice revealed that MHC^{b} haplotype is responsible for higher responsiveness to LPS, compared with MHC^{d} haplotype (22). However, the molecular mechanism by which the *TLR4* gene determines high or low responsiveness to LPS has not yet been addressed.

In this study, we dissected B cell activation using agonistic mAbs against TLR4 (26) and RP105 (16), in addition to LPS. Use of these agonistic mAbs provides a distinct advantage, because cross talk with TLR family members other than TLR4 and RP105 because of contaminated pathogen-derived stimulants is negligible. Furthermore, these Abs enable specific analysis of activation via TLR4 and RP105, respectively. In this article, we demonstrate that the low LPS responsiveness of BALB B cells is attributed to TLR4, but not to RP105 signals, and is due to decreased expression of surface TLR4. Molecular analysis revealed that a V254I mutation impaired surface expression of TLR4. These findings will facilitate studies to uncover the mechanism(s) of genetic control of LPS sensitivity and also to reveal the mechanism of directing TLR4 to the proper subcellular compartment.

Materials and Methods

Animals and cells

B6 and BALB mice and Wistar rats were obtained from Charles River Japan (Yokohama, Japan). *MD-2*$^{-/-}$ (6) and *RP105*$^{-/-}$ (5) mice were previously established in our laboratory. *TLR4*$^{-/-}$ mice (4) were a gift from Dr. S. Akira (Osaka University, Osaka, Japan). The animals were maintained and bred at the Animal Facility, Saga Medical School, under a 12 h/12 h light/dark photoperiod, and given food and water ad libitum. All animal experiments were done in accordance with the Saga Medical School guidelines for the care and treatment of animals used in experimentation.

Human embryonic kidney HEK293 (CRL-1573), mouse myeloma SP2/O (CRL-1581), and rat NRK-52E (CRL-1571) cell lines were purchased from the American Type Culture Collection (Rockville, MD). HEK293, NRK-52E, and derivative transfected cells were maintained in DMEM supplemented with 10% FCS. SP2/O cells and derivative hybridoma clones were maintained in RPMI 1640 medium supplemented with 10% FCS and 50 μM 2-ME. Ba/F3 and derived transfected cells were maintained as previously described (5).

Reagents and Abs

LPS from *E. coli ATCC 25922* was prepared as described previously (27). Phosphorothioate-stabilized CpG oligonucleotide (5′-TCCATGACGTTCCTGATGCT-3′) was purchased from Hokkaido System Science (Sapporo, Japan). Anti-TLR4 (UT12, UT49) (26) and anti-PR105 (RP/16) (16) mAbs were prepared as previously described. Rat anti-human CD14 mAb (1B12) was established in our laboratory, as described previously (28, 29). In brief, two Wistar rats were immunized in the foot pads with human CD14-expressing NRK-52E transfected cells (2×10^7/head) emulsified in CFA in a total volume of 1.5 ml. One week later, cells were harvested from the draining lymph nodes of the immunized rats. The harvested cells were fused with SP2/O myeloma cells in polyethylene glycol 1500. After HAT selection, positive hybridoma clones were screened by immunofluorescence staining against HEK293 transfected cells expressing human CD14, and single clones were isolated by limiting dilution. Purified mAb was obtained from ascitic fluids of SCID mice by caprylic acid precipitation followed by DEAE ion exchange chromatography. Other Abs were purchased from the following companies: FITC-labeled anti-B220 and PE-conjugated anti-CD69 mAbs from eBiosciences (San Diego, CA); FITC-labeled anti-CD11b, -CD11c, and -CD19 and PE-conjugated anti-CD3ε mAbs from BioLegend (San Diego, CA); PE-conjugated anti-CD86 and -CD138 mAbs and PE-conjugated streptavidin (stv) from BD Biosciences (San Jose, CA); and PE-conjugated goat anti-mouse IgG Ab from Southern Biotechnology Associates (Birmingham, AL). Biotinylated (Bio)-mAbs were prepared using EZ-Link NHS-LC-Biotin (Pierce, Rockford, IL), according to the manufacturer's instructions.

Cell staining and flow cytometric analysis

Cells were stained at 4°C with primary mAbs or Bio-mAbs in staining buffer (HBSS containing 2% FCS, and 0.1% sodium azide for splenocytes and Ba/F3-derived cells; PBS containing 3% FCS, 10 mM EDTA, and 0.1% sodium azide for HEK293-derived cells, resident macrophages, bone marrow–derived macrophages [BMMs], and bone marrow–derived dendritic cells [BMDCs]). After washing three times, cells were incubated with PE-conjugated stv or goat anti-mouse IgG and subjected to flow cytometric analysis using a FACScan or FACSCalibur (Becton Dickinson, Franklin Lakes, NJ). Collected data were analyzed by the WinMDI program (J. Trotter, The Scripps Research Institute, La Jolla, CA).

MTT assay

Murine splenocytes ($2–5 \times 10^5$ cells) were stimulated in 100 μl on 96-well plates. After a 3-d stimulation, 25 μl MTT (5 mg/ml; Sigma, St. Louis, MO) was added to the cells for an additional 5 h, and the resultant precipitates were dissolved in acidified isopropanol containing 10% Triton X-100. OD measurements were made at 540 and 650 nm using a SpectraMax microplate reader (Molecular Devices LLC, Sunnyvale, CA). Cell growth was calculated by subtracting OD_{650} values from OD_{540} values.

Real-time PCR for quantification of TLR4 and MD-2 mRNA

B220^{+} B cells were isolated from splenocytes using *Pan*-B Dynabeads (Invitrogen, Carlsbad, CA), according to the manufacturer's instructions. Total RNA was isolated using the RNeasy mini kit (Qiagen, Valencia, CA) with on-column DNase treatment and reverse transcribed to cDNA using Superscript-II (Invitrogen). *TLR4*, *MD-2*, and *β-actin* cDNA were detected using SYBR Premix ExTaq (Takara, Shiga, Japan). Primers used were the following: 5′-CAGCCTGAGACACTTAGACCTCAGC-3′ and 5′-GAACGCTGAGAATTCTGTGACCC-3′ for *TLR4*; 5′-GTGGTTCTGCAACTCCTCCGATGC-3′ and 5′-CATGTCCATGGCACAGAACTTCC-3′ for *MD-2*; 5′-TGCGTGACATCAAAGAGAAG-3′ and 5′-CGGATGTCAACGTCACACTT-3′ for *β-actin*. Real-time PCR was performed using an ABI PRISM 7000 Sequence Detection System (Applied Biosystems, Carlsbad, CA). The mRNA levels were determined using standard curves prepared by plotting defined amounts of plasmids containing the target gene against its respective threshold cycle. Levels of *TLR4* and *MD-2* mRNA were normalized to that of *β-actin* mRNA. Specific amplification was confirmed by running the products on agarose gels by electrophoresis.

Construction of expression vectors

A panel of TLR4 expression vectors was constructed as follows: cDNA fragments coding for the N-terminal (aa 1–438, TLR4N) and C-terminal (aa 439–835, TLR4C) halves of TLR4 were amplified from cDNA purified from B6 or BALB B cells by PCR using the primers 5′-ccaatcgatgcagaaaatgccaggATGATG-3′ and 5′-GAACGCTGAGAATTCTGTGACCC-3′ for TLR4N, and 5′-GGGTCACAGAATTCTCAGCGTTC-3′ and 5′-tttgcggccgcTCAGGTCCAAGTTGCCG-3′ for TLR4C, respectively. TLR4N and TLR4C fragments were cloned into pBluescript II-KS(+) at ClaI and EcoRI sites (TLR4N/pBSKS) and at EcoRI and NotI sites (TLR4C/pBSKS), respectively. B6 and BALB TLR4N fragments were further subcloned into either B6 or BALB TLR4C/pBSKS at KpnI and EcoRI sites to obtain full-length *TLR4* (TLR4/pBSKS). TLR4/pBSKS was digested with SalI and NotI, and then subcloned into a pEFBOS vector at XhoI and NotI sites. Resultant vectors (TLR4/pEFBOS) expressed B6, BALB, B6/BALB, or BALB/B6 TLR4 (see later) by changing the combination of B6 and BALB TLR4N and TLR4C sequences. M209I and V254I TLR4 expression vectors were constructed by site-directed mutagenesis as follows: M209I and V254I mutations were introduced into B6 TLR4N/pBSKS using the primers 5′-CTCTCTTTAGACATaTCTTTGAACCC-3′ and 5′-GGGTTCAAAGAtATGTCTAAAGAGAG-3′, and 5′-GCTGGTTTACACaTCCATCGGTTGATCTTG-3′ and 5′-CAAGATCAACCGATGGAtGTGTAAACCAGC-3′, respectively. Mutated TLR4N fragments were subcloned into the B6 TLR4C/pEFBOS vector at ClaI and HpaI sites. Full-length mouse *TLR2* without a stop codon was amplified from an EST clone (accession no. BE916892; Open Biosystems, Livermore, CA) by PCR using the primers 5′-aacctcgagccgaaacctcagacaaagcg-

3′ and 5′-gagagatctGGACTTTATTGCAGTTCTC-3′. The PCR product was digested with XhoI and BglII, and subcloned into a pEFBOS vector, which was modified by introducing a FLAG tag at the C terminus, and at XhoI and compatible BamHI sites. A resultant vector expresses TLR2 tagged with FLAG at the C terminus. Full-length human *CD14* was subcloned from an EST clone (accession no. BC010507; Open Biosystems) into pBluescript II-KS(+) at EcoRI and NotI sites. This insert was further subcloned into a pEFBOS vector at XhoI and NotI sites. Full-length mouse *MD-2* was subcloned into a pCAGGS1 vector from a MD-2/pEFBOS vector (30) at XhoI and NotI sites.

Transfection study

In transient transfection experiments, TLR4/pEFBOS constructs were co-transfected into HEK293 cells with a pEFBOS vector containing human CD14 (as a transfection control) in the presence or absence of a pEFBOS vector containing mouse MD-2 (30) using Lipofectamine 2000 (Invitrogen). After 24–48 h cultivation, surface expression of TLR4 and CD14 was determined by flow cytometry. To establish stably transfected cells, TLR4/pEFBOS constructs were transfected into HEK293 cells with pBabePuro selection vectors using Lipofectamine 2000. After puromycin selection, stably transfected clones were screened by flow cytometry using UT49 or another TLR4 mAb, as described previously (26). Ba/F3 reporter cells carrying NF-κB–responsive luciferase gene (5) were transfected with a TLR4/pEFBOS construct with a MD-2/pCAGGS1 construct by the electroporation with GenePulser (Bio-Rad, Hercules, CA). After G418 selection, stably transfected clones were obtained as described earlier.

NF-κB reporter assay

Ten thousand Ba/F3-transfected cells carrying TLR4/MD-2/NF-κB reporter gene were stimulated with LPS for 5 h, and luciferase activity was measured as previously described (29).

Preparation of resident macrophage

Resident macrophages were collected by peritoneal lavage with ice-cold PBS, washed twice, and then suspended in staining buffer.

Generation of BMMs and BMDCs

BMMs and BMDCs were generated from bone marrow cells that were prepared from femurs and tibias, and subjected to RBC-lysis in a hypotonic solution (0.15 M NH_4Cl, 1.0 mM $KHCO_3$, and 0.1 mM Na_2EDTA) as previously described (6) with slight modification. For BMM, bone marrow cells (1×10^7) were cultured in 10 ml DMEM containing 10% FCS and 10% L929-conditioned medium (CM) as a source of M-CSF on 10-cm petri dish. Ten percent of L929-CM was replenished on day 4. After 7-d cultivation, BMM was collected by ice-cold PBS containing 1 mM EDTA and subjected to FACS analysis. BMMs ($0.5–1 \times 10^5$) were stimulated with LPS or UT12 for 21 h in 200 μl culture medium without L929-CM in a 96-well plate.

To generate BMDCs, we cultured bone marrow cells (1×10^6) in RPMI 1640 containing 10% FCS, 50 μM 2-ME, and 1% CM from CHO cells stably expressing GM-CSF on 24-well plate with replacement of culture medium on days 2 and 4. On day 6, loosely attached BMDCs were collected and subjected to FACS analysis. BMDCs (1×10^5) were stimulated in the absence of GM-CSF as done in BMMs.

ELISA

Concentration of TNF-α in cell culture supernatant and serum was determined by a Mouse TNF-α ELISA Ready-SET-Go! kit (eBiosciences), according to the manufacturer's instructions.

Endotoxic shock model

Mice were i.p. injected with sublethal dose of UT12 (5 μg/head), and serum was collected 3 d before and 1 and 3 h after the challenge. Seven days later, RBC-lysed spleen cells were stained and subjected to flow cytometry.

Results

TLR4 and RP105 induce B cell activation without mutual interaction

In B cells, both TLR4 and RP105 receptors were reported to function in response to LPS (4, 5). To dissect the individual roles of TLR4 and RP105 in LPS-induced B cell activation, we examined the impact of agonistic mAbs against TLR4 (UT12) and RP105 (RP/16) on splenocytes from $TLR4^{-/-}$ and $PR105^{-/-}$ mice. UT12 and RP/16 both induced proliferation of $RP105^{-/-}$ and $TLR4^{-/-}$ splenocytes, respectively, comparable with that of wild-type (wt) B cells (Fig. 1A). Consistent with this, upregulation of CD69 and CD86 in $RP105^{-/-}$ and $TLR4^{-/-}$ splenic B cells was

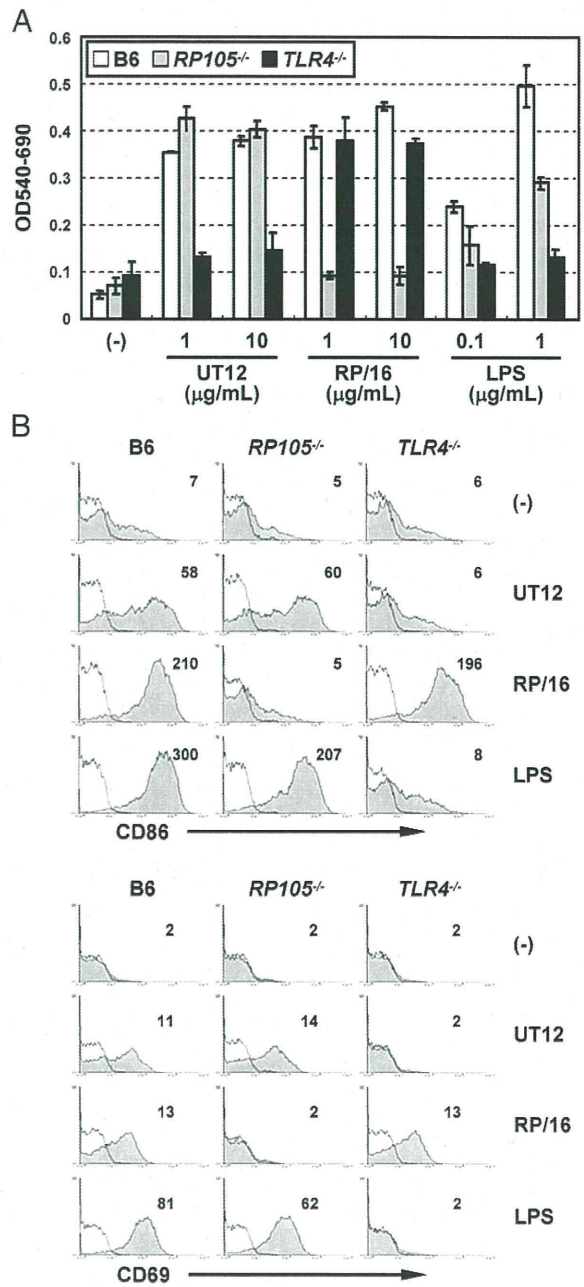

FIGURE 1. TLR4 and RP105 induce B cell activation without mutual interaction. (**A**) Splenocytes from wt B6 (white columns), $RP105^{-/-}$ (gray columns), or $TLR4^{-/-}$ (black columns) mice were stimulated with anti-TLR4 mAb (UT12), anti-RP105 mAb (RP/16), or LPS at the indicated concentrations (μg/ml) for 3 d. Cell proliferation was determined by MTT assay. Data are shown as the mean ± SD from triplicate cultures. Similar results were obtained from three independent experiments. (**B**) Splenocytes were stimulated with UT12 (10 μg/ml), RP/16 (10 μg/ml), or LPS (1 μg/ml) for 24 h and then stained with PE-conjugated CD69 or CD86 and FITC-conjugated B220 mAbs. The expression of CD69 and CD86 on $B220^+$ B cells was assessed by flow cytometry. Open histogram represents staining without PE-conjugated mAb. Mean fluorescence intensity (MFI) of CD69 and CD86 staining is depicted in the histograms. Results are representative of two independent experiments.

induced by UT12 and RP/16, respectively, to a similar degree as seen in wt B6 B cells (Fig. 1B). *TLR4*$^{-/-}$ and *RP105*$^{-/-}$ splenocytes were unresponsive to UT12 and RP/16 stimulation. These results indicated that TLR4 and RP105 activated B cells without mutual interaction.

Impaired TLR4 signaling in BALB B cells compared with that in B6 B cells

BALB B cells were reported to be less responsive to LPS than B6 B cells (21, 22). To reveal whether the different sensitivity is attributable to TLR4- or RP105-mediated signaling, we compared the response of B6 and BALB B cells with UT12 and RP/16 (Fig. 2A, 2B). UT12-induced proliferation and upregulation of CD69 and CD86 was clearly decreased in BALB B cells. In contrast, RP/16-induced responses of BALB B cells were similar or slightly higher than those of B6 B cells. These findings indicate that strain-dependent differences in LPS responsiveness were due to TLR4-specific signals. Furthermore, we tested B cell responses to a TLR9 agonist, CpG, to reveal whether other TLR signals were also decreased in BALB B cells. We found that CpG was a good stimulator of both B6 and BALB B cells, which resulted in robust proliferation and upregulation of CD69 (Fig. 2C, 2D).

Impaired cell-surface expression of BALB TLR4

Considering the comparable responses to CpG of these mouse strains, we thought it unlikely that signaling events that are common among TLRs were impaired in BALB B cells. Therefore, we hypothesized that the low responsiveness of BALB B cells to LPS could be caused by decreased amounts of cell-surface TLR4 molecules. To test this possibility, we compared *TLR4* mRNA levels in purified B cells by real-time PCR. However, its expression level in BALB B cells was comparable with that in B6 B cells (Fig. 3A). Next, we compared surface expression levels of TLR4 by flow cytometry. In general, surface TLR4 levels on B cells are known to be too low to detect by flow cytometry. However, among the TLR4 mAbs we tested, TLR4 was clearly detected with UT49 (Fig. 3B). Consistent with our speculation, surface TLR4 in BALB B cells was lower than that in B6 B cells (Fig. 3B). We confirmed the specificity of this staining using *TLR4*$^{-/-}$ mice to exclude the possibility that this signal resulted from nonspecific binding to other cell-surface molecules (Fig. 3B). Following these observations, we further questioned the dependency of TLR4 surface expression on MD-2 using *MD-2*$^{-/-}$ mice. It was found that *MD-2*$^{-/-}$ B cells expressed slightly lower levels of TLR4 on their cell surface compared with wt B6 B cells (Fig. 3B). There was no difference in *MD-2* mRNA levels between B6 and BALB B cells (Fig. 3A). These results suggest that surface TLR4 levels were decreased in BALB B cells because of posttranscriptional mechanisms, and that B cells do not necessarily require MD-2 for TLR4 targeting to the cell surface, just as macrophages and dendritic cells do not (11, 13). Because RP105 expression was reported to be controlled by MHC haplotype (22), we also compared its expression level in B cells. However, we were unable to observe the extremely low surface RP105 expression. The level in BALB B cells appeared similar or slightly lower than that in B6 B cells (Fig. 3C).

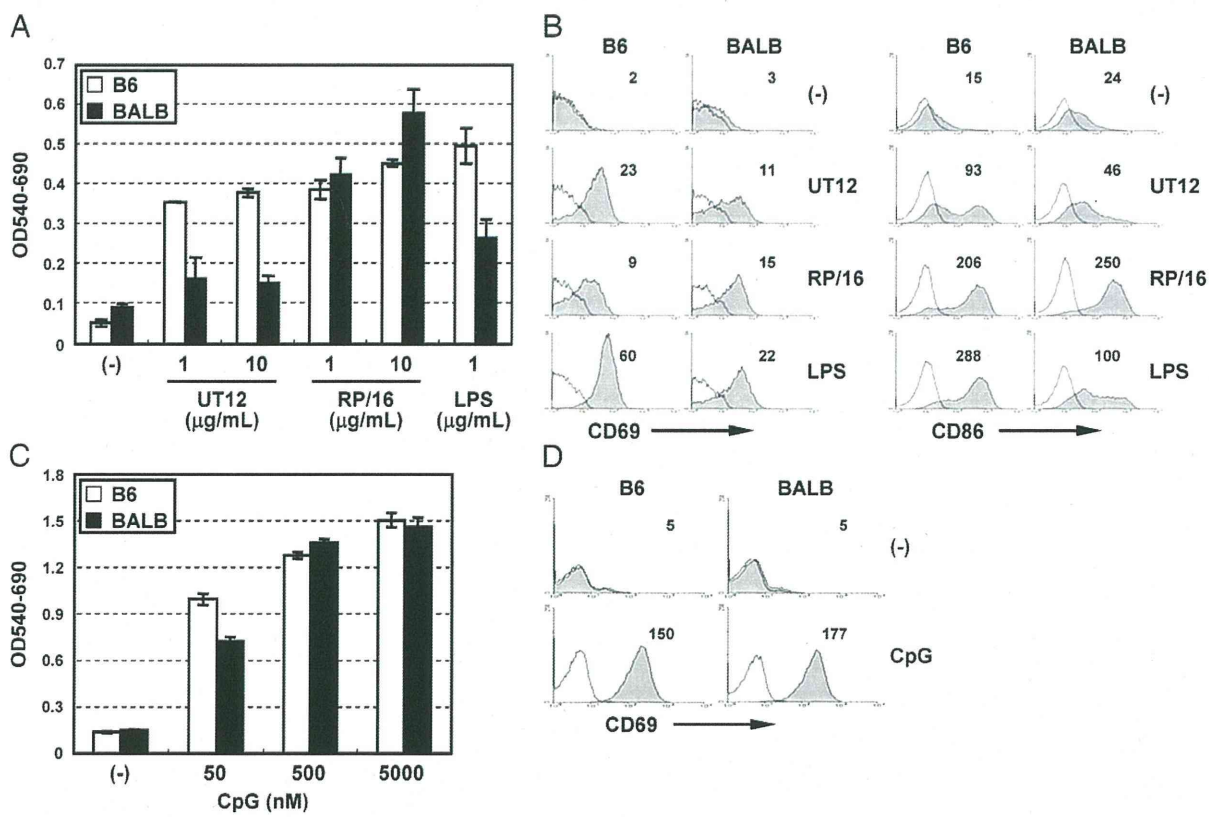

FIGURE 2. Impaired TLR4 signaling in BALB B cells compared with that in B6 B cells. (**A** and **C**) Splenocytes from B6 (white columns) or BALB (black columns) mice were stimulated with (A) UT12, RP/16, or LPS (μg/ml) for 3 d or (C) CpG (μM) for 2 d at the indicated concentrations. Cell proliferation was determined as in Fig. 1A. Similar results were obtained in eight (A) and two (C) independent experiments. (**B** and **D**) Splenocytes were stimulated with (B) UT12 (10 μg/ml), RP/16 (10 μg/ml), or LPS (1 μg/ml) or (D) CpG (1 μM) for 24 h and then stained with PE-conjugated CD69 or CD86 mAb in the presence of FITC-conjugated B220 mAb. The expression of CD69 and CD86 on B220^{+} B cells was analyzed by flow cytometry. Open histogram represents staining without PE-conjugated mAb. MFI of staining was depicted in the histograms. Results are representative of four (B) and two (D) independent experiments.

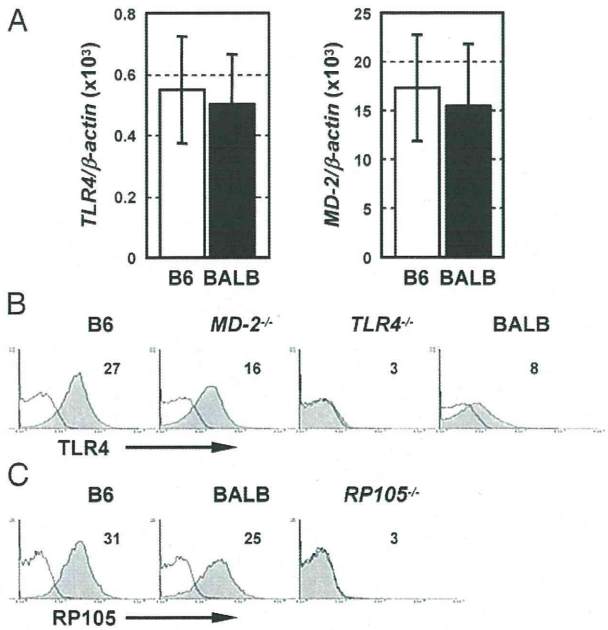

FIGURE 3. Impaired cell-surface expression of BALB TLR4 in B cells. (**A**) The expression of *TLR4* and *MD-2* mRNA in $B220^+$ B cells purified from B6 (white columns) or BALB (black columns) splenocytes was determined by quantitative real-time PCR. The level of *TLR4* (*left panel*) and *MD-2* (*right panel*) mRNA was normalized to that of *β-actin* mRNA. Data are shown as the mean ± SD of B cells from five mice. Measurements were conducted twice with similar results. (**B**) Splenocytes from wt, *MD-2*$^{-/-}$, or *TLR4*$^{-/-}$ B6 or wt BALB mice were stained with Bio-UT49 (anti-TLR4) and FITC-conjugated B220 mAbs followed by PE-stv. The expression of TLR4 on $B220^+$ B cells was analyzed by flow cytometry. Open histogram represents staining with a Bio-isotype control. Numbers indicate MFI of Bio-UT49 staining. Results are representative of three to seven mice in two independent experiments. (**C**) Splenocytes from wt or *RP105*$^{-/-}$ B6 or wt BALB mice were stained with Bio-RP/16 and FITC-conjugated B220 mAbs followed by PE-stv. The expression of RP105 on $B220^+$ B cells was analyzed as in (B). Similar results were obtained from two independent experiments.

A V254I mutation in BALB TLR4 impairs surface TLR4 expression

There are six genetic variations between the B6 and BALB *TLR4*-coding sequences (Fig. 4A) (31). Four of these cause amino acid changes (M209I, V254I, E593D, and R761H). The other two are synonymous mutations (N575N and N715N). We cotransfected either B6 or BALB TLR4 expression constructs with a CD14 construct (as a control to monitor transfection efficiency) into HEK293 cells to reveal whether decreased expression was intrinsic to the *TLR4*-coding sequence. As shown in Fig. 4B, BALB TLR4-transfected HEK293 cells showed lower expression than B6 TLR4-transfected cells when stained with the UT49 mAb. In contrast, there were no prominent differences in the expression level of surface CD14, indicating similar transfection efficiencies among the transfected cells. This suggests that decreased surface expression of BALB TLR4 was attributable to the *TLR4*-coding sequence. To reveal which variation(s) in particular affected cell-surface expression of TLR4, we constructed a panel of mutated TLR4 expression constructs (Fig. 4A) and transfected them into HEK293 cells. As shown in Fig. 4B and Supplemental Fig. 1, expression of B6 TLR4 with the M209I and V254I mutations (BALB/B6 TLR4) was comparable with that of BALB TLR4, whereas expression of B6 TLR4 with the N575N, E593D, N719N, and R761H mutations (B6/BALB TLR4) was clearly higher than that of BALB TLR4. This indicated that either M209I or V254I (or both) was the responsible single nucleotide polymorphism (SNP) for decreased expression of BALB TLR4. Therefore, we further examined the contribution of both M209I and V254I to decreased TLR4 by introducing site-specific mutations into B6 TLR4. The V254I mutation clearly caused decreased B6 TLR4 expression, comparable with BALB TLR4 levels, whereas the M209I mutation did not. Similar findings were obtained in stably transfected HEK293 cells expressing B6, M209I, V254I, and BALB TLR4 (Fig. 4C). These findings suggest that V254I was the mutation responsible for impaired surface expression of BALB TLR4.

Surface expression of and signaling by transfected BALB TLR4 is lower compared with B6 TLR4 even in the presence of MD-2

MD-2 has been reported to enhance cell-surface TLR4 expression (11, 12), although it is dispensable in HEK293 cells (11). *MD-2*$^{-/-}$ B6 B cells expressed slightly lower surface TLR4 levels (Fig. 3B). Therefore, we performed a transfection study in which MD-2 was transduced into B6 or BALB TLR4 stably transfected cells to clarify whether MD-2 could rescue lower surface BALB TLR4 expression. As previously demonstrated (11), MD-2 transfection enhanced BALB TLR4 surface expression. However, the higher BALB TLR4 level was still lower than B6 TLR4 expression (Fig. 5A, Supplemental Fig. 2). To confirm this, we cotransfected varying amounts of MD-2 constructs together with the B6 or BALB TLR4 construct (Fig. 5B, Supplemental Fig. 3). Cotransfection of MD-2 dose dependently increased BALB TLR4 expression. However, the absolute expression levels of BALB TLR4 remained lower than B6 TLR4 levels at all concentrations of MD-2 construct. The transfection efficiency, monitored by CD14 expression, was consistent in these experiments. In addition, we confirmed that BALB TLR4 expression level is still lower than B6 TLR4 level when they are stably transfected in Ba/F3 cells together with MD-2 and NF-κB reporter gene (Fig. 5C). These findings indicate that MD-2 could not fully rescue surface BALB TLR4 expression to the level seen with B6 TLR4 and support the notion that low expression of TLR4 in BALB B cells is due to the V254I mutation in the BALB TLR4 sequence. Together with these findings, we performed NF-κB reporter assay and revealed that BALB TLR4-transfected Ba/F3 cells were hyporesponsive to LPS stimulation compared with B6 TLR4-transfected cells (Fig. 5D). These results suggest that V254I mutation is a mechanism to account for low LPS responder phenotypes of BALB B cells.

Slightly impaired TLR4 expression and signaling in BALB dendritic cells, but not in macrophages

To extend our findings, we examined cell-surface expression of B6 versus BALB TLR4 on other immune cell types such as BMDCs, BMMs, and resident macrophages. Reduced TLR4 expression level was observed in BALB BMDCs as observed in B cells (Fig. 6A). Consistent with this, the responses of BALB BMDCs to LPS and UT12 were lower than those of B6 BMDCs as assessed by TNF-α secretion (Fig. 6B). In contrast with B cells and BMDCs, we could not see any strain difference in TLR4 expression and responses to LPS and UT12 in resident macrophage and BMM (Fig. 6C–E). Therefore, V254I mutation in *TLR4* gene appears not always to confer low responsiveness on all cell types.

BALB mice have similar sensitivity to endotoxic shock but impaired plasma cell differentiation

We examined the sensitivity to endotoxic shock in vivo by administrating agonistic UT12 mAb and measuring serum TNF-α. It was found that endotoxic shock was induced with similar degree

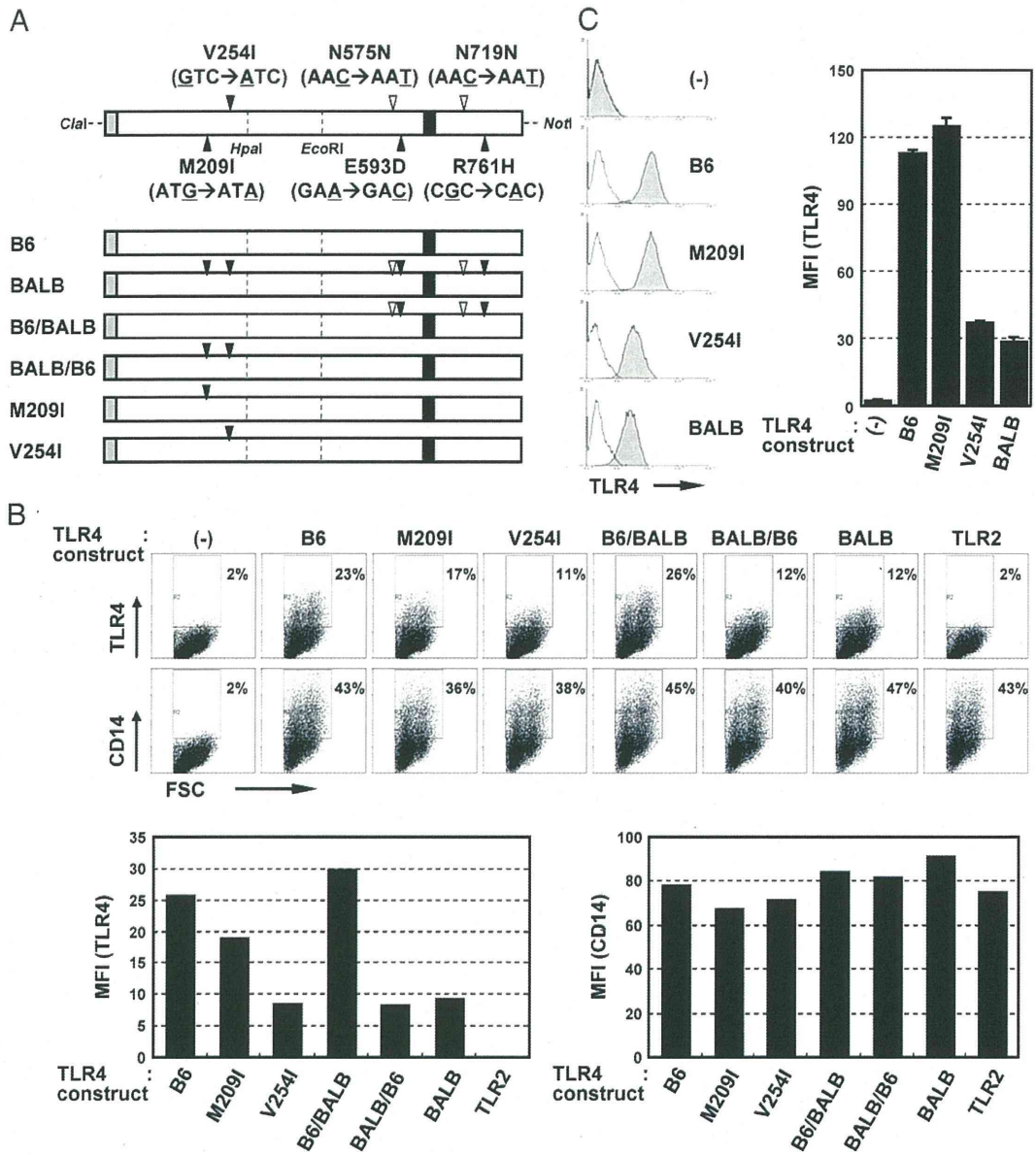

FIGURE 4. A V254I mutation in BALB TLR4 impairs surface TLR4 expression. (**A**) Scheme for the panel of TLR4 expression constructs. There are six SNPs between B6 and BALB *TLR4*-coding sequences. Four of these cause amino acid substitutions (M209I, V254I, E593D, and R761H; black arrowheads) in B6 TLR4. The other two variations are synonymous mutations (N575N and N715N; open arrowheads). The gray and white regions represent the signal peptide and the B6 TLR4 mature sequence, respectively. The block region represents the transmembrane domain. HpaI and EcoRI sites used for subcloning are indicated by a dotted line. (**B**) TLR4 constructs were cotransfected into HEK293 cells with a construct expressing human CD14. After 24- to 48-h cultivation, surface expression of TLR4 and CD14 was determined by flow cytometry using Bio-UT49 for TLR4 and Bio-1B12 for CD14 followed by PE-stv. A TLR2 expression vector was transfected as a negative control. Data are represented as the MFI of each transfected cell type in the gated regions by subtracting that of nontransfected cells. Percentage of gated cells was depicted in dot plot. Results are representative of three similar independent experiments (Supplementary Fig. 1). (**C**) Stable HEK293-transfected clones expressing B6, M209I, V254I, or BALB TLR4 were analyzed by flow cytometry using Bio-UT49 for TLR4 followed by PE-stv. Open histograms represent staining without Bio-mAbs. The data are summarized as mean ± SD MFI from three independent clones, as in (B). Similar results were obtained in three independent experiments.

between B6 and BALB mice (Fig. 7A). In this experiment, we unexpectedly found that UT12-injected mice have enlarged spleen at least because of the increased B cell and $CD138^+$ plasma cell numbers (Fig. 7B). This massive B cell proliferation was more obvious in B6 mice than in BALB mice, a finding that proves that TLR4 signaling in BALB B cells is still impaired in vivo as demonstrated in vitro.

Discussion

By using agonistic mAbs to TLR4 and RP105, we revealed that susceptibility to LPS in murine B cells was genetically controlled by signals from TLR4, not from RP105. B6 B cells showed stronger responses to agonistic anti-TLR4 mAb than BALB B cells, as assessed by proliferation and upregulation of CD69 and CD86, whereas the responses to agonistic anti-RP105 mAb were slightly lower or similar rather than higher in B6 B cells. We also demonstrated by flow cytometry that the surface TLR4 level in B6 B cells was higher than that in BALB B cells. NF-κB reporter assay showed that BALB TLR4-transfected Ba/F3 cells were hyporesponsive to LPS stimulation than B6 TLR4-transfected cells in concordance with decreased surface expression. Because surface TLR4 levels are related to the magnitude of the LPS response